Hepatocytes Buried in the Cirrhotic Livers of Patients With Biliary Atresia Proliferate and Function in the Livers of Urokinase-Type Plasminogen Activator–NOG Mice

Hiroshi Suemizu,[1]* **Kazuaki Nakamura,**[3]* **Kenji Kawai,**[2] **Yuichiro Higuchi,**[1] **Mureo Kasahara,**[4] **Junichiro Fujimoto,**[5] **Akito Tanoue,**[3] and **Masato Nakamura**[6]

[1]Biomedical Research Department, and [2]Pathology Research Department, Central Institute for Experimental Animals, Kanagawa, Japan; [3]Department of Pharmacology, [4]Department of Transplant Surgery, and [5]Clinical Research Center, National Center for Child Health and Development, Tokyo, Japan; and [6]Department of Pathology and Regenerative Medicine, Tokai University School of Medicine, Kanagawa, Japan

The pathogenesis of biliary atresia (BA), which leads to end-stage cirrhosis in most patients, has been thought to inflame and obstruct the intrahepatic and extrahepatic bile ducts. BA is not believed to be caused by abnormalities in parenchymal hepatocytes. However, there has been no report of a detailed analysis of hepatocytes buried in the cirrhotic livers of patients with BA. Therefore, we evaluated the proliferative potential of these hepatocytes in immunodeficient, liver-injured mice [the urokinase-type plasminogen activator (uPA) transgenic NOD/Shi-scid IL2rγnull (NOG); uPA-NOG strain]. We succeeded in isolating viable hepatocytes from the livers of patients with BA who had various degrees of fibrosis. The isolated hepatocytes were intrasplenically transplanted into the livers of uPA-NOG mice. The hepatocytes of only 3 of the 9 BA patients secreted detectable amounts of human albumin in sera when they were transplanted into mice. However, human leukocyte antigen–positive hepatocyte colonies were detected in 7 of the 9 mice with hepatocyte transplants from patients with BA. We demonstrated that hepatocytes buried in the cirrhotic livers of patients with BA retained their proliferative potential. A liver that was reconstituted with hepatocytes from patients with BA was shown to be a functioning human liver

with a drug-metabolizing enzyme gene expression pattern that was representative of mature human liver and biliary function, as ascertained by fluorescent dye excretion into the bile canaliculi. These results imply that removing the primary etiology via an earlier portoenterostomy may increase the quantity of functionally intact hepatocytes remaining in a cirrhotic liver and may contribute to improved outcomes. *Liver Transpl 20:1127-1137, 2014*. © 2014 AASLD.

Biliary atresia (BA), the most common pediatric cholestatic disease, is caused by the progressive fibro-obliterative obstruction of the extrahepatic and intrahepatic bile ducts within the first few weeks of life.[1,2] The current surgical treatment is sequential. In the first few weeks of life, a Kasai portoenterostomy is performed to bypass the obstructed extrahepatic bile ducts and restore the biliary flow.[3] Approximately 20% of all patients who undergo portoenterostomy during infancy survive into adulthood with their native liver.[2,4] In general, it is advantageous to perform portoenterostomy as early after birth as possible to optimize the chance of success.[5] Patients who fail to undergo portoenterostomy experience a gradual deterioration of liver function and develop progressive fibrosclerosis; after the initial successful establishment of bile flow, liver transplantation (LT) is the only treatment option. Although several etiologies of BA have been postulated, the precise pathogenesis of BA remains unknown. Some factors that might contribute to its development are genetic, infective, inflammatory, and toxic insults.[1] In most cases, BA is associated with an intensive inflammatory infiltrate; this knowledge led us to the conjecture that BA results from an infectious or autoimmune destruction of the bile ducts. For example, the infection of newborn mice with the Rhesus rotavirus results in a BA-like disease.[6-8] Meanwhile, hepatocytes from patients with BA have not been thought to be involved in the development of chronic obstructive cholestasis. We and other groups have developed mice with humanized livers in which the liver is reconstituted with human hepatocytes so that in vivo drug metabolism and liver regeneration can be studied.[9-11] Therefore, the aims of this study were to evaluate the in vivo proliferative potential and functional properties of hepatocytes buried in the cirrhotic livers of BA patients.

MATERIALS AND METHODS

Specimens from the National Research Institute for Child Health and Development were collected in a standardized manner with the permission of the patients' families.

Animals

All mouse studies were conducted in strict accordance with *Guide for the Care and Use of Laboratory Animals* from the Central Institute for Experimental Animals. All experimental protocols were approved by the animal care committee of the Central Institute for Experimental Animals (permit number 11029A). All surgeries were performed under isoflurane anesthesia, and all efforts were made to minimize animal suffering. All studies using mouse tissue with transplanted human cells were approved by the ethics and biosafety committee of the National Research Institute for Child Health and Development and the Central Institute for Experimental Animals. The urokinase-type plasminogen activator (uPA) transgenic NOD/Shi-scid IL2rγnull (NOG); uPA-NOG strain[11] was maintained through the breeding of a female uPA-NOG hemizygote with a male homozygote. The zygosity of the *uPA* transgene was presumed from the degree of liver damage, which was examined through the determination of the serum levels of alanine aminotransferase with a Fuji DRI-CHEM 7000 clinical biochemical analyzer (Fujifilm Corp., Tokyo, Japan). The uPA-NOG mice with serum alanine aminotransferase activity greater than 150 U/L were selected as homozygotes and were then used as transplant recipients.

Isolation of Hepatocytes From the Livers of Patients With BA

The entire experimental protocol was approved by the ethics and research committee of the National Center for Child Health and Development. Written informed consent was obtained in each case. Except for the pieces of liver tissue that were used as pathological specimens, the enucleated diseased livers from the transplant recipients were discarded. The human hepatocytes used in this study were procured from liver tissue removed from BA patients who met the diagnostic criteria [Pediatric End-Stage Liver Disease (PELD) score[12] ≥ 6 points] for LT operations. The levels of fibrosis were categorized according to the following criteria: (I) mild (portal fibrous expansion to bridging fibrosis involving ≤50% of portal tracts), (II) moderate (bridging fibrosis involving >50% of portal tracts), and (III) severe (bridging fibrosis involving >50% of the portal tracts with nodular architectural changes).[13] Patient 141, who had grade III fibrosis and a PELD score of 0, had portopulmonary syndrome (intrapulmonary shunting). The shunt ratio, calculated with technetium-99m macroaggregated albumin (ALB) scintigraphy, was 16.8%, which indicated a relatively mild shunt. The hepatocytes were isolated from the resected liver tissue through the 2-step collagenase perfusion[14] of the liver samples, as described previously.[15] Hepatic parenchymal cells were isolated with low-speed centrifugation (50*g*). Cell numbers and viability were assessed with trypan blue exclusion.[16]

Flow Cytometry Analysis

The hepatocytes were stained with 1 mg/mL propidium iodide (PI; Sigma-Aldrich Co. LLC, St. Louis, MO), which stains dead cells. The intensity of 502-nm fluorescence was measured as intrinsic fluorescence (IF). Flow cytometry data were collected with a FACSCanto analyzer and BD FACSDiva software (BD Biosciences, Franklin Lakes, NJ). The data were analyzed with the FlowJo program (Tree Star, Inc., Ashland, OR).

Transplantation of Hepatocytes Into uPA-NOG Mice

Hepatocytes from patients with BA and commercially available cryopreserved human hepatocytes from a 4-year-old female (NHEPS, Lonza, Walkersville, MD) were used as donor cells. Young (8-week-old) male uPA-NOG mice were used as the recipients of the human hepatocytes. One million viable hepatocytes were injected intrasplenically via a Hamilton syringe with a 26-G needle. The successful engraftment of the human hepatocytes was evaluated through the measurement of the blood level of human albumin (hALB) with an hALB enzyme-linked immunosorbent assay quantitation kit (Bethyl Laboratories, Montgomery, TX) according to the manufacturer's protocol. The replacement index, which was the percentage of human donor hepatocytes in the recipient liver, was estimated according to the hALB concentration in chimeric mice.[17]

Histology and Immunohistochemistry

The tissues were fixed with 4% (vol/vol) phosphate-buffered formalin (Mildform, Wako Pure Chemical Industries, Ltd., Osaka, Japan), and 5-μm paraffin-embedded sections were stained with Azan-Mallory staining reagents (Muto Pure Chemicals, Tokyo, Japan) to visualize the collagen and muscle fibers and with hematoxylin and eosin (H&E). Some sections were autoclaved for 10 minutes in a target retrieval solution [0.1 M citrate buffer (pH 6.0) and 1 mM ethylene diamine tetraacetic acid (pH 9.0)] and were then equilibrated at room temperature for 20 minutes. Monoclonal mouse anti–human leukocyte antigen (anti-HLA) class I (A-C) antibodies (clone EMR8-5, Hokudo, Sapporo, Japan; 1:2000),[18] polyclonal goat anti-human ALB antibodies (Bethyl Laboratories; 1:1500), polyclonal rabbit anti-cytochrome P450 3A4 (CYP3A4) antibodies (Abcam, Inc., Cambridge, MA; 1:500), monoclonal mouse anti-human Ki-67 antigen antibodies (clone MIB-1; Dako Denmark A/S; 1:50),[19] monoclonal mouse anti-human multidrug resistance–associated protein 2 (MRP2) antibodies (clone M2 III-6, Millipore, Billerica, MA; 1:100),[20] monoclonal rabbit anti-vimentin (anti-VIM) antibodies (clone SP20, Nichirei Bioscience, Tokyo, Japan; 1:1500),[21] and monoclonal rabbit anti–alpha smooth muscle actin (anti-αSMA) antibodies (clone 1A4, Leica Microsystems, Tokyo, Japan; 1:200)[22] were used as primary antibodies. Normal mouse serum (NMS), normal goat serum (NGS), and normal rabbit serum (NRS) were used as negative controls for immunostaining. For bright-field immunohistochemistry, the antibodies for mouse, goat, and rabbit immunoglobulin were visualized with amino acid polymer/peroxidase complex–labeled antibodies [Histofine Simple Stain MAX PO (M, G, and R), Nichirei Bioscience) and a Bond Polymer Refine Detection system (Leica Microsystems) with a diaminobenzidine substrate [Dojindo Laboratories, Kumamoto, Japan; 0.2 mg/mL 3,3′-diaminobenzidine tetrahydrochloride, 0.05 M tris(hydroxymethyl)-aminomethane with hydrochloric acid (pH 7.6), and 0.005% hydrogen peroxide]. The sections were counterstained with hematoxylin. Hepatic biliary obstructions were examined with Hall's bilirubin staining method.[23] The images were captured under an Axio Imager upright microscope (Carl Zeiss, Thornwood, NY) equipped with AxioCam HRm and AxioCam MRc5 charge-coupled device cameras (Carl Zeiss).

Real-Time Quantitative Reverse-Transcription Polymerase Chain Reaction for Drug Metabolism–Related Gene Expression

The total cellular RNA was isolated from the livers with an RNeasy mini kit (Qiagen K.K.). Complementary DNA was synthesized with a high-capacity complementary DNA reverse transcription kit (Applied Biosystems, Foster City, CA) with random hexamers. TaqMan gene expression master mix and TaqMan gene expression assays (Applied Biosystems) were used for the real-time quantitative polymerase chain reactions; amplifications were performed with an ABI-Prism 7000 sequence detection system (Applied Biosystems). The comparative threshold cycle (Ct) method was used to determine the relative ratio of the gene expression for each gene, which was corrected with human glyceraldehyde-3-phosphate dehydrogenase (GAPDH) and referenced to the RNA extracted from donor hepatocytes. The TaqMan assay numbers are listed in Table 1.

Biliary Excretion Test With 5(6)-Carboxyfluorescein Diacetate (5-CFDA)

The ester precursor of 5-carboxyfluorescein (5-CF), 5(6)-carboxyfluorescein diacetate (5-CFDA; 0.5 nmol; Sigma-Aldrich), was injected intravenously into the mouse tail vein. Ten minutes after the 5-CFDA injection, the liver was perfused with 50 nmol/L 5-CFDA for 3 minutes, and the liver was then embedded in an optimum cutting temperature (O.C.T.) compound (Sakura Finetek Japan Co., Ltd., Tokyo, Japan) and frozen in liquid nitrogen. Ten-micrometer-thick serial frozen sections were prepared and air-dried. The 5-CF fluorescent signals were captured with an Axio Imager upright microscope (Carl Zeiss) equipped with AxioCam HRm and AxioCam MRc5 charge-coupled device cameras (Carl Zeiss). After the microfluorographs were taken, the tissue sections were fixed and rehydrated sequentially in decreasing concentrations of ethanol and water, and this was followed by immunohistochemical staining for MRP2. Sections were counterstained with

	TABLE 1. TaqMan Probe Information	
Gene Name	Gene Description	TaqMan Assay Number
GAPDH	Glyceraldehyde-3-phosphate dehydrogenase	Hs99999905_m1
ALB	Albumin	Hs99999922_s1
CYP1A1	Cytochrome P450, family 1, subfamily A, polypeptide 1	Hs00153120_m1
CYP1A2	Cytochrome P450, family 1, subfamily A, polypeptide 2	Hs00167927_m1
CYP2A6	Cytochrome P450, family 2, subfamily A, polypeptide 6	Hs00868409_s1
CYP2B6	Cytochrome P450, family 2, subfamily B, polypeptide 6	Hs03044634_m1
CYP2C8	Cytochrome P450, family 2, subfamily C, polypeptide 8	Hs00258314_m1
CYP2C9	Cytochrome P450, family 2, subfamily C, polypeptide 9	Hs00426397_m1
CYP2C18	Cytochrome P450, family 2, subfamily C, polypeptide 18	Hs00426400_m1
CYP2C19	Cytochrome P450, family 2, subfamily C, polypeptide 19	Hs00426380_m1
CYP2D6	Cytochrome P450, family 2, subfamily D, polypeptide 6	Hs00164385_m1
CYP2E1	Cytochrome P450, family 2, subfamily E, polypeptide 1	Hs00559368_m1
CYP3A4	Cytochrome P450, family 3, subfamily A, polypeptide 4	Hs00430021_m1
CYP3A5	Cytochrome P450, family 3, subfamily A, polypeptide 5	Hs00241417_m1
UGT1A1	Uridine diphosphate glucuronosyltransferase 1 family, polypeptide A1	Hs02511055_s1
UGT2B15	Uridine diphosphate glucuronosyltransferase 2 family, polypeptide B15	Hs00870076_s1
ABCB1	Adenosine triphosphate–binding cassette, subfamily B (MDR/TAP), member 1	Hs00184500_m1
ABCB11	Adenosine triphosphate–binding cassette, subfamily B (MDR/TAP), member 11	Hs00184824_m1
ABCC2	Adenosine triphosphate–binding cassette, subfamily C (CFTR/MRP), member 2	Hs00166123_m1
ABCG2	Adenosine triphosphate–binding cassette, subfamily G (WHITE), member 2	Hs01053790_m1
SLC22A1	Solute carrier family 22 (organic cation transporter), member 1	Hs00427552_m1
SLC22A7	Solute carrier family 22 (organic anion transporter), member 7	Hs00198527_m1
SLC22A9	Solute carrier family 22 (organic anion transporter), member 9	Hs00971064_m1
NR1H4	Nuclear receptor subfamily 1, group H, member 4	Hs00231968_m1
NR1I2	Nuclear receptor subfamily 1, group I, member 2	Hs00243666_m1
NR1I3	Nuclear receptor subfamily 1, group I, member 3	Hs00901571_m1

hematoxylin. Another tissue section was fixed in 4% paraformaldehyde, and this was followed by immunofluorescent staining with monoclonal mouse anti-HLA class I (A-C) antibodies, a streptavidin/Texas Red–labeled secondary antibody (GE Healthcare Bio-Sciences), and H&E. Commercially available cryopreserved human hepatocytes (normal hepatocytes) and cells from the HCT 116 line (American Type Culture Collection, Manassas, VA), a human colorectal carcinoma cell line that easily engrafts and forms tumor cell colonies in NOG mouse livers,[24] were used as positive and negative controls for the formulation of the bile canaliculus (BC) network.

Statistical Analyses

Group comparisons were performed with the Student t test for independent samples. P values less than 0.05 were considered significant (Prism 5, GraphPad Software, Inc., La Jolla, CA).

RESULTS

Engraftment of Hepatocytes From Patients With BA in uPA-NOG Mouse Livers

Using liver failure immunodeficient mouse models, we first evaluated the regenerative potential of the residual hepatocytes buried in the cirrhotic livers of patients with BA.[11] We succeeded in isolating viable hepatocytes from the livers of 9 BA patients with various degrees of fibrosclerosis (Table 2 and Fig. 1A). The typical gross morphology of a liver from a patient with BA is shown in Fig. 1B. There was no significant difference ($P = 0.45$) between the cell yields from patients with grade II fibrosis (2.3 ± 1.6 million cells per gram of liver, n = 3) and patients with grade III fibrosis (3.8 ± 4.2 million cells per gram of liver, n = 6; Fig. 1C). The cell viability was not significantly different ($P = 0.81$) between patients with grade II fibrosis ($76.7\% \pm 16.0\%$, n = 3) and patients with grade III fibrosis ($73.3\% \pm 23.0\%$, n = 6; Fig. 1D). The isolated hepatocytes were analyzed with flow cytometry (Fig. 1D). Because the IF signal of the hepatocytes from patients with BA was not increased in comparison with normal hepatocytes, it did not seem that bile accumulated within the hepatocytes, even in the patients with BA. The viable and engraftable hepatic parenchymal cells seemed to be present in the high intrinsic fluorescence (HIF) fraction; these cells had a very large cell mass and a complicated internal structure because the percentage of the HIF fraction correlated positively with the engraftability of the hepatocytes, which was based on the plasma concentration of hALB ($r^2 = 0.8784$; Fig. 1E, right). However, the cell viability did not show a direct correlation with the plasma concentration of hALB ($r^2 = 0.0515$; Fig. 1E, center) or the percentage of the HIF fraction ($r^2 = 0.0064$; Fig. 1E, left). The isolated hepatocytes were intrasplenically transplanted into uPA-NOG mice. Successful engraftment was evaluated in terms of the detection of hALB in the mouse serum

TABLE 2. Engraftment of Hepatocytes Derived From Patients With BA in uPA-NOG Mouse Livers

| | | | | | Patient Information | | | Experimental Condition and Summarized Results | | | |
| | | | | | Isolated Hepatocytes | | | | | Animals With Engraftment | |
Number	Age	Sex	Fibrosis Level	PELD Score	Cells/g of Liver	Viability (%)	HIF (%)	Condition*	Cell Dose (Cells/Mouse)	HLA-Positive Colony [n/N (%)]†	hALB [n/N (µg/mL)]
80	10 months	Female	II	20	1.2×10^6	66	9.0	A	1.0×10^6	5/5 (100)	5/5 (230-875)
								B	1.0×10^6	4/4 (100)	1/4 (280)
								C	1.0×10^6	4/4 (100)	1/4 (38)
86	7 months	Female	II	35	1.5×10^6	95	4.8	A	1.0×10^6	2/2 (100)	1/2 (35)
								B	1.0×10^6	2/4 (50)	1/4 (105)
153	8 months	Male	II	9	4.1×10^6	69	1.3	B	1.0×10^6	2/3 (67)	0/3 (ND)
105	5 months	Female	III	13	1.2×10^7	83	8.5	B	1.0×10^6	4/4 (100)	4/4 (49-294)
133	6 months	Female	III	15	6.9×10^4	33	9.2	B	2.0×10^5	0/1 (0)	0/1 (ND)
141	12 years	Female	III	0	3.0×10^6	93	4.8	B	1.0×10^6	1/1 (100)	0/1 (ND)
149	8 months	Female	III	14	3.4×10^6	67	0.8	B	1.2×10^6	3/3 (100)	0/3 (ND)
151	5 months	Female	III	10	1.4×10^6	69	5.0	B	1.0×10^6	3/4 (75)	0/4 (ND)
154	6 months	Female	III	14	3.1×10^6	95	4.2	B	1.0×10^6	0/1 (0)	0/1 (ND)
77	32 years	Male	Normal	—	2.0×10^6	88	25.5	C	1.0×10^6	5/5 (100)	5/5 (35-1516)

*The conditions were as follows: (A) fresh hepatocytes (within the first 6 hours after isolation), (B) chilled hepatocytes (stored at 4°C for more than 16 hours and up to 24 hours), and (C) cryopreserved hepatocytes.
†Hepatocyte colonies that contained more than 20 HLA-positive cells in the cross-sections.

and the appearance of HLA-positive hepatocyte colonies in the liver tissue (Fig. 1F). Although detectable amounts of secreted hALB were found only in the sera of mice that had received hepatocyte transplants from 3 of the 9 BA patients, HLA-positive hepatocyte colonies were detected as a result of 7 of the 9 hepatocyte transplants from patients with BA.

The expression of drug-metabolizing enzymes, a marker of a fully matured liver, was analyzed with real-time quantitative polymerase chain reaction. Livers reconstituted with hepatocytes from 2 different patients with BA (patients 80 and 105) and commercially available cryopreserved hepatocytes (NHEPS) were then examined. The relative gene expression profiles of hepatocytes from patients with BA were similar to those of NHEPS hepatocytes (Fig. 1G). The expression levels of most of the genes were higher in the reconstituted livers versus the donor hepatocytes (Fig. 1H).

Next, we examined the expression of ALB, a major functional marker of biosynthesis in the liver, via immunohistochemical staining with human-specific antibodies in hepatocytes originating from patients with BA (Fig. 2A, top and middle). This hepatic lineage marker protein was expressed within the human hepatocyte colonies in the reconstituted-liver mice at levels comparable to those of the liver reconstituted with cryopreserved normal hepatocytes (patient 77; Fig. 2A, bottom). The expression of CYP3A4, which is the main drug-metabolizing enzyme found in the liver, was also observed within the colonies consisting of both hepatocytes from patients with BA (Fig. 2A, top and middle) and normal hepatocytes (Fig. 2A, bottom), but it did not show the zonal distribution observed in the fully reconstituted uPA-NOG liver with NHEPS hepatocytes (Fig. 2B). Most human hepatocytes originating from the patients with BA were present as small foci that appeared to grow by clonal expansion within the uPA-NOG mouse livers. This growth was quite similar to that of normal hepatocytes from patient 77. In addition, immunohistochemical nuclear staining of serial sections of the mouse livers with an antibody (MIB-1) against the human Ki-67 antigen[25,26] revealed that the proliferative potential of the hepatocytes from the patients with BA was preserved, as evidenced by the nuclear staining of the hepatocytes located at the edges of human hepatocyte colonies (Fig. 2A, top and middle). NGS, NRS, and NMS (nonimmune), which corresponded to the host animals in which anti-ALB, anti-CYP3A4, and anti–Ki-67 antibodies, respectively, were prepared, did not react with either human or mouse hepatocytes (Fig. 2C). The hepatocyte colonies derived from the patients with BA were not stained by Azan-Mallory staining (Fig. 2A, top and middle).

Functional Integrity of Partially Humanized Livers

We confirmed the expression of MRP2 proteins on the plasma membranes of hepatocytes in both the livers of patients with BA and the partially humanized livers repopulated with hepatocytes from patients with BA
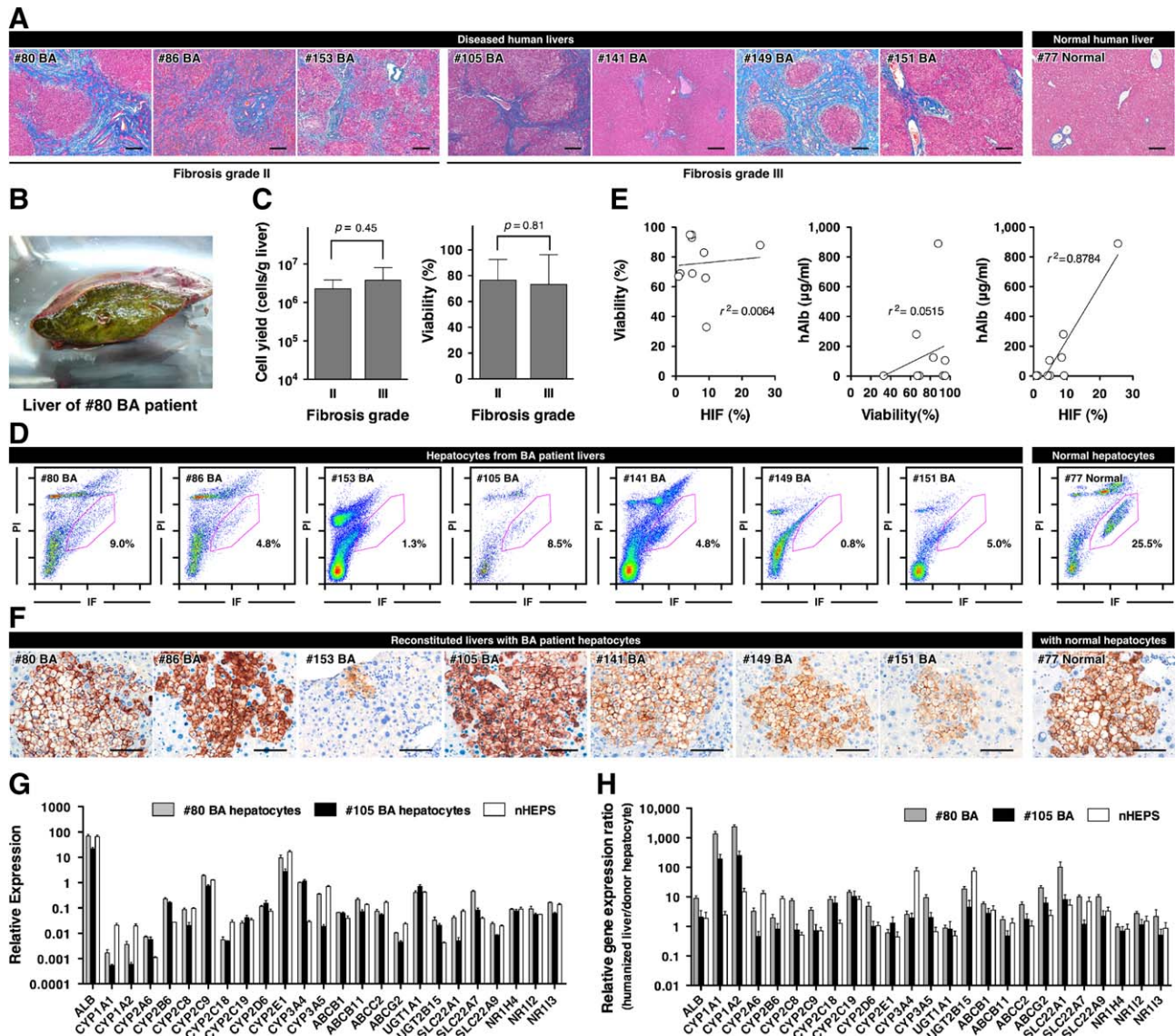
Figure 1. Engraftment of hepatocytes from BA patients in uPA-NOG mouse livers. (A) Azan-Mallory staining of 7 individual liver biopsy samples from BA patients and a healthy donor (normal). The scale bars represent 200 μm. (B) Gross morphology of the liver from BA patient 80. (C) Comparison of the cell yields and viability with grade II hepatic fibrosis and grade III hepatic fibrosis. (D) Isolated hepatocytes were analyzed with flow cytometry. Each HIF fraction is surrounded by a magenta border. (E) Correlation analyses of the cell viability, the HIF fraction percentage, and the hALB plasma concentration. (F) The engraftment of hepatocytes isolated from the BA patients and the healthy donors was confirmed with anti-human HLA staining. The scale bars represent 50 μm. (G) The relative expression levels of 24 human drug metabolism–related messenger RNAs in hepatocytes from BA patients and NHEPS hepatocytes were corrected with GAPDH. (H) The relative ratio of the gene expression for each reconstituted liver was referenced to the RNA extracted from the donor hepatocytes.

(Fig. 3A,B,). The cholestasis, visualized with Hall's bilirubin staining, was observed in many BCs in the livers of patients with BA (Fig. 3A, right). In contrast, the colonies repopulated with hepatocytes from patients with BA within the host mouse livers did not accumulate bile within their BCs (Fig. 3B). Azan-Mallory staining and VIM and αSMA antibody staining revealed fibrosis in the livers of patients with BA (Fig. 3C), but no fibrosis was observed within the colony repopulated with hepatocytes from patients with BA (Fig. 3D). We wondered whether these hepatocytes could reconstitute the functionally integrated BC net-

work within the host mouse liver; therefore, we assessed the transporter function within the colonies of hepatocytes from patients with BA with 5-CFDA, a fluorescent marker used to visualize biliary excretion into BCs. After it is administered, 5-CFDA enters hepatocytes and is metabolized into 5-CF. This compound is excreted into BCs through the organic anion transporter MRP2.[27] Within the first 15 minutes after the administration of 5-CFDA, the hepatocytes from patients with BA in the uPA-NOG mice excreted 5-CF into the BCs, and it formed honeycomb networks surrounding individual hepatocytes (Fig. 4, top). This
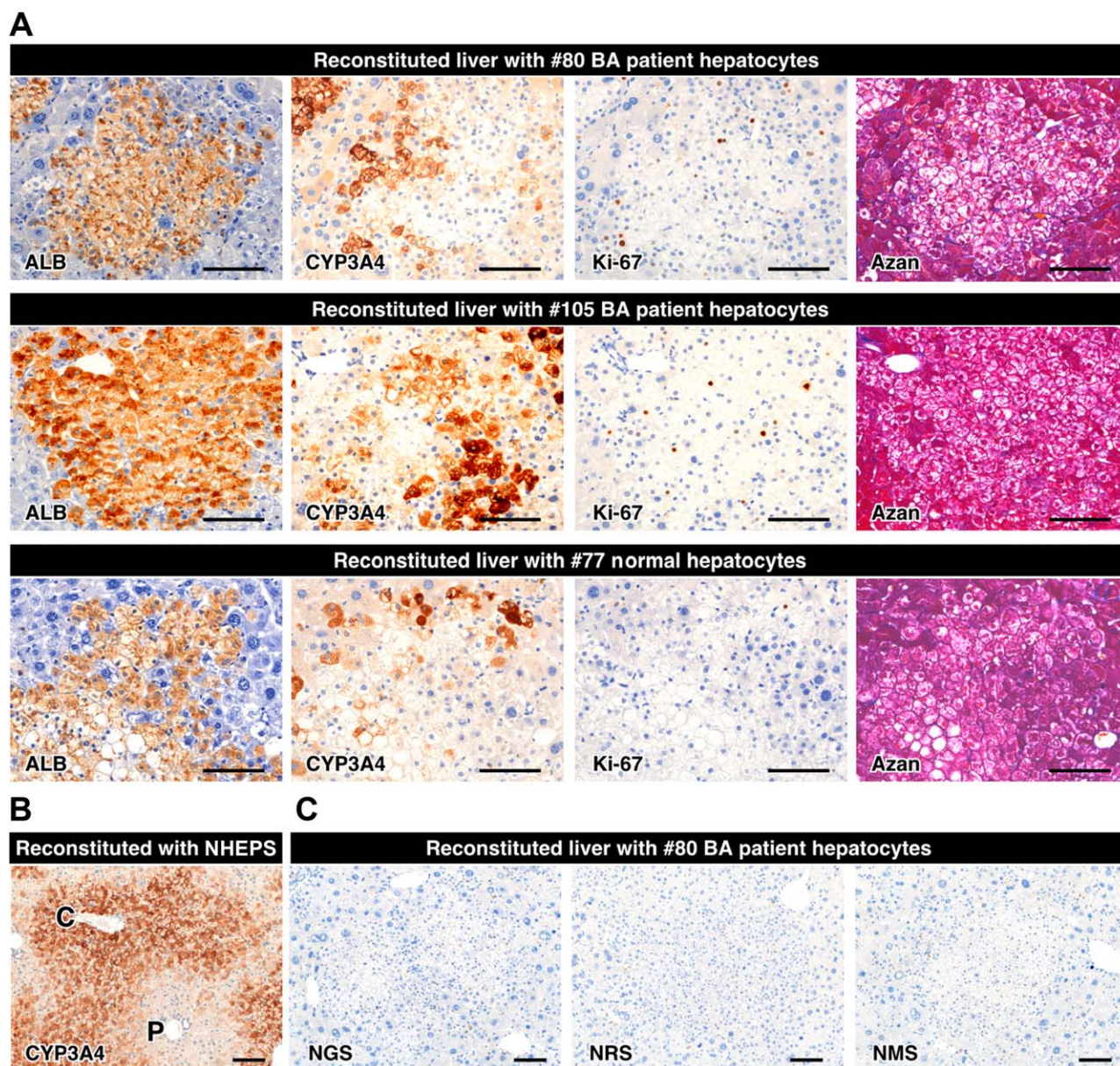
Figure 2.   Immunohistochemistry of uPA-NOG mouse livers engrafted with BA patient hepatocytes. (A) Sections were stained for hALB, human CYP3A4, and human Ki-67 antigen; Azan-Mallory staining was also used. The scale bars represent 100 μm. (B) Immunohistochemical staining for CYP3A4 in a fully reconstituted uPA-NOG liver with NHEPS hepatocytes. The scale bar represents 100 μm. (C) Negative controls for immunostaining: NGS, NRS, and NMS. The scale bars represent 100 μm.

process was also observed in the colonies of NHEPS hepatocytes (Fig. 4, middle) but not in the HCT 116 colorectal tumors (Fig. 4, bottom). The typical BC network was detectable in the human hepatocyte conglomerates, as visualized by anti-MRP2, HLA antibodies, and H&E staining (Fig. 4). These results suggest that the intrahepatic bile duct system within the colonies reconstituted with hepatocytes from patients with BA must be nondefective.

DISCUSSION

BA is the most common reason for LT in children worldwide. The aim of this study was to evaluate

regenerative medicine as a possible alternative to LT for treating BA. We succeeded in isolating viable hepatocytes from the livers of patients with BA so that we could evaluate the regenerative potential in vivo with a liver failure mouse model.[11] Recently, Gramignoli et al.[28] reported the successful isolation of hepatocytes from people with a number of different metabolic and other liver diseases (n = 35). The purpose of their study was to evaluate hepatocytes from individuals with metabolic disease for use in cell therapy via hepatocyte transplantation. Although they performed hepatocyte isolation in patients with BA (n = 7), those cells would not be recommended for clinical transplants because of concerns about cell yields, viability,
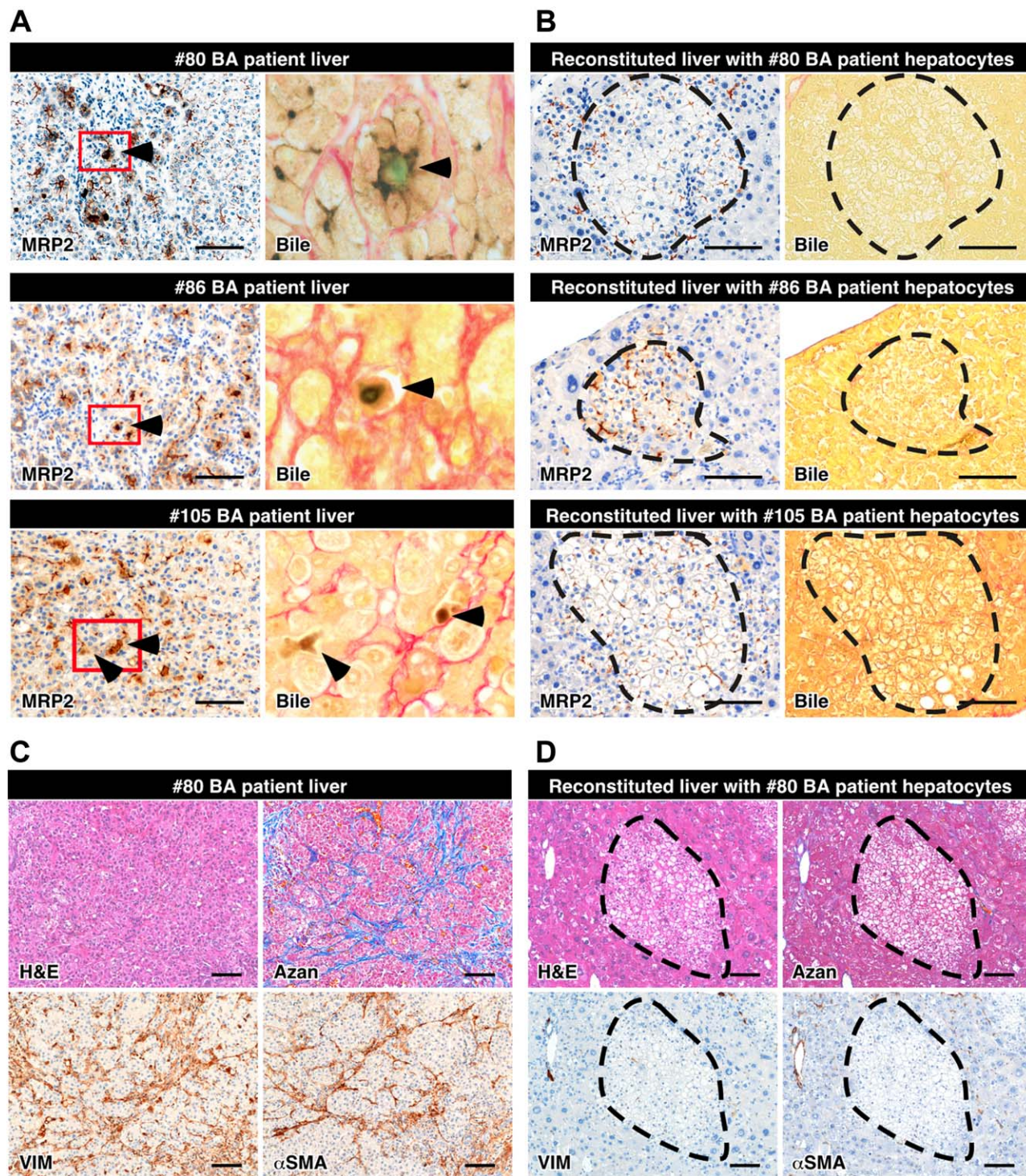
Figure 3.   Detection of biliary obstructions and hepatic fibrosis. (A) Immunohistochemical staining for MRP2 protein in livers from patients with BA (patients 80, 86, and 105; left). Enlarged views of the boxed areas are shown with Hall's bilirubin staining (right). Bile stained with Hall's method appears green (arrowheads). (B) Immunohistochemical staining for MRP2 protein (left) and Hall's bilirubin staining (right) in uPA-NOG mouse livers engrafted with hepatocytes from BA patients (patients 80, 86, and 105). The dotted areas indicate the repopulated human liver. (C) H&E and Azan-Mallory staining and immunohistochemical staining for VIM and αSMA in the liver from a BA patient (patient 80). (D) H&E and Azan-Mallory staining and immunohistochemical staining for VIM and αSMA in a uPA-NOG mouse liver engrafted with hepatocytes from a BA patient (patient 80). The dotted areas indicate the repopulated human liver. The scale bars represent 100 μm.
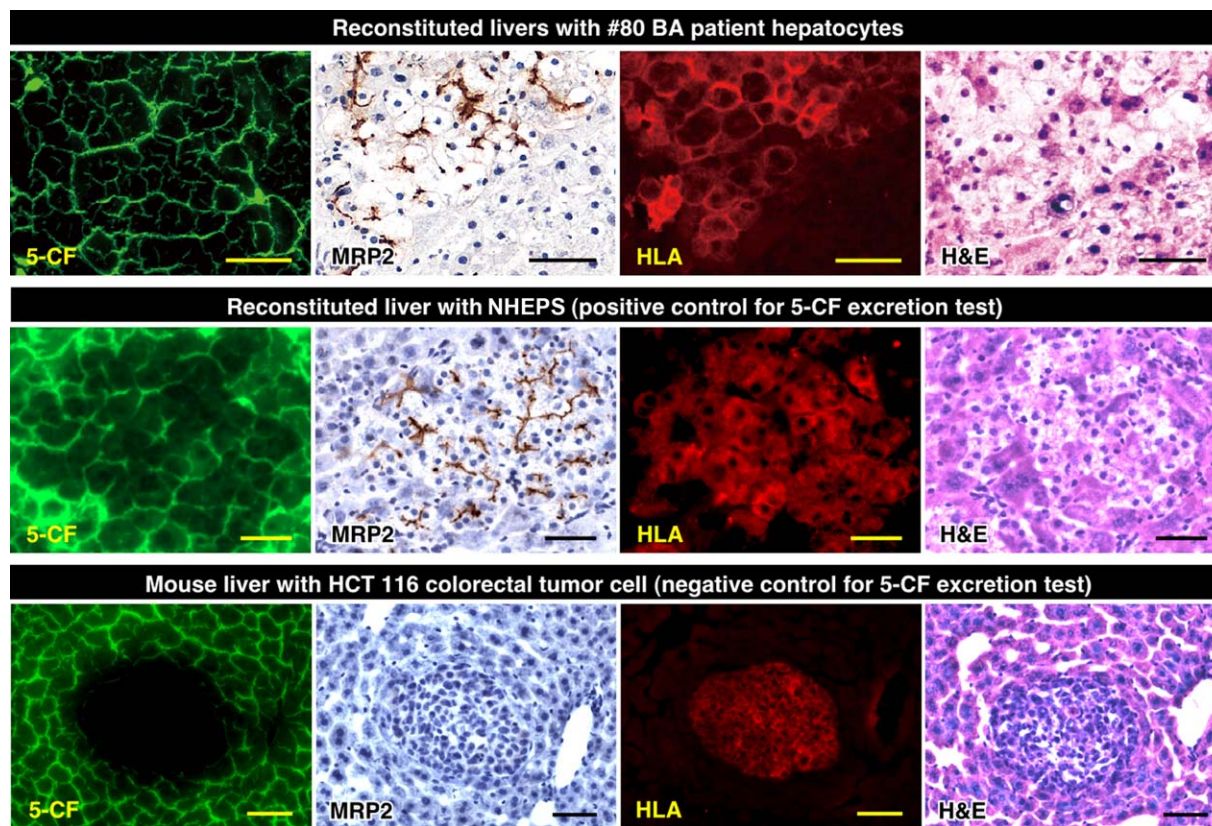
Figure 4.   Functional integrity of the BC network within the reconstituted livers. Biliary excretion tests were performed with a fluorescent metabolic marker (5-CFDA). Serial sections were prepared from the livers of mice that received transplants of hepatocytes from a BA patient (patient 80), commercially available cryopreserved hepatocytes (NHEPS; positive control), or HCT 116 colorectal tumor cells (negative control). The sections were loaded with 5-CFDA, and the presence of the fluorescent metabolite 5-CF was assessed. In the livers reconstituted with patient hepatocytes and NHEPS hepatocytes, 5-CF (green on a dark field) was rapidly excreted into the BCs that formed the honeycomb networks over the lobule. In contrast, the BCs around the tumor, which formed after the transplantation of HCT 116 colorectal tumor cells, did not have this honeycomb pattern. Additional sections were stained for human MRP2 (brown in a bright field) and HLA (red in a dark field); H&E staining was also performed. The scale bars represent 50 μm.

and function. Bhogal et al.[29] reported that the viability, the total cell yield, and the success rate with cirrhotic tissues were low. In the current study, the cell yield and cell viability of hepatocytes from BA patients with fibrosis grade II or III were comparable to the yields and viability previously reported by Gramignoli et al. We expected that the low cell yield and viability would depend on the degree of fibrosis in patients with BA. However, there were no significant differences in the cell yields of hepatocytes from patients with grade II fibrosis and hepatocytes from patients with grade III fibrosis (Fig. 1C) or in cell viability (Fig. 1D). These results indicate that regardless of the extent of hepatic fibrosis, the presence of fibrosis affects the cell yield and viability when hepatocytes are isolated from the livers of patients with BA.

For hepatocytes from patient 80, 3 different conditions (freshly isolated, chilled, and frozen-thawed hepatocytes) were compared in terms of their engraftment and proliferative potential in a liver failure model using uPA-NOG mice. HLA-positive hepatocyte colonies were observed in the livers of all uPA-NOG mice that underwent transplantation with hepatocytes

of any condition; however, a higher ratio of hALB-secreting mice and a higher level of serum hALB were observed in the mice that underwent transplantation with freshly isolated hepatocytes (Table 2). We succeeded in isolating a small number of hepatocytes buried in the severely cirrhotic liver of BA patient 149 (fibrosis grade III), and surprisingly, the hepatocytes could successfully engraft and proliferate within the uPA-NOG mouse livers as HLA-positive colonies. These results indicate that even hepatocytes buried in the cirrhotic livers of patients with BA do not lose their proliferative potential.

Recent studies of the molecular biology of BA have revealed no significant differences in the hepatic MRP2 expression levels of BA patients and control groups.[30] In fact, we confirmed the expression of not only the adenosine triphosphate–binding cassette, subfamily C (cystic fibrosis transmembrane conductance regulator (CFTR)/multidrug resistance-associated protein (MRP)), member 2 (ABCC2) gene but also the MRP2 protein, which was located on the apical plasma membranes of hepatocytes both in the livers of BA patients (Fig. 3A, left) and in partially humanized livers repopulated with hepatocytes from patients

with BA (Fig. 3B, left). Despite the normal MRP2 protein expression in the livers of patients with BA and in the partially humanized mouse liver, the bile was accumulated only in the many BCs of livers from patients with BA. This result clearly demonstrates the extrahepatic obstruction of the biliary flow.

In this study, using a reconstituted-liver mouse model, we examined the hepatocytes of patients with BA for the presence of abnormalities in vivo. Unfortunately, we failed to establish a BA model with liver-injured mice. However, this result indicates that the primary etiology of BA is absent in the hepatocytes themselves, and the hepatocytes buried in the cirrhotic livers of patients with BA are functionally intact hepatocytes retaining their proliferative potential and able to reconstitute a partially functioning human liver in mice. Gramignoli et al.[28] recently reported the isolation of hepatocytes from patients with many metabolic diseases, including BA, and the rapid and efficient repopulation of FRG (fumarylacetoacetate hydrolase (Fah), recombination activating gene 2 (Rag2) and interleukin 2 receptor gamma chain (Il-2rγ) triple gene knockout) mouse livers after the transplantation of hepatocytes obtained from patients with metabolic disease. In addition to Gramignoli et al.'s report, the current study supports the hypothesis that hepatocytes from patients with BA are morphologically and biochemically normal.

Recently, it has been reported that the extent of liver fibrosis at the time of portoenterostomy, as evaluated by picrosirius red staining, appears to be a strong negative predictor of outcomes.[31] The negative correlation between the extent of liver fibrosis and the yield of viable hepatocytes suggested by our results might be associated with that phenomenon. These results support the possibility that if the primary etiology is removed by Kasai portoenterostomy before progressive cholestasis develops, the liver of the patient with BA may regenerate autologously via the functionally intact hepatocytes remaining in the cirrhotic liver. The hepatocyte function in patients with BA may be independent of the degree of fibrosis; therefore, efforts to ameliorate the fibrosis would have great promise in treating this disease. Treatment would include an earlier diagnosis and surgery but might also include developing antifibrotic pharmacological approaches. If a method for earlier diagnosis or new drugs are developed in the near future, patients with BA may not require an operation that is as difficult as LT.

ACKNOWLEDGMENT

REFERENCES

1. Hartley JL, Davenport M, Kelly DA. Biliary atresia. Lancet 2009;374:1704-1713.
2. Bassett MD, Murray KF. Biliary atresia: recent progress. J Clin Gastroenterol 2008;42:720-729.
3. Muratore CS, Harty MW, Papa EF, Tracy TF Jr. Dexamethasone alters the hepatic inflammatory cellular profile without changes in matrix degradation during liver repair following biliary decompression. J Surg Res 2009; 156:231-239.
4. Sokol RJ, Shepherd RW, Superina R, Bezerra JA, Robuck P, Hoofnagle JH. Screening and outcomes in biliary atresia: summary of a National Institutes of Health workshop. Hepatology 2007;46:566-581.
5. Serinet MO, Wildhaber BE, Broué P, Lachaux A, Sarles J, Jacquemin E, et al. Impact of age at Kasai operation on its results in late childhood and adolescence: a rational basis for biliary atresia screening. Pediatrics 2009;123: 1280-1286.
6. Czech-Schmidt G, Verhagen W, Szavay P, Leonhardt J, Petersen C. Immunological gap in the infectious animal model for biliary atresia. J Surg Res 2001;101:62-67.
7. Petersen C, Biermanns D, Kuske M, Schäkel K, Meyer-Junghänel L, Mildenberger H. New aspects in a murine model for extrahepatic biliary atresia. J Pediatr Surg 1997;32:1190-1195.
8. Riepenhoff-Talty M, Schaekel K, Clark HF, Mueller W, Uhnoo I, Rossi T, et al. Group A rotaviruses produce extrahepatic biliary obstruction in orally inoculated newborn mice. Pediatr Res 1993;33(pt 1):394-399.
9. Dandri M, Burda MR, Török E, Pollok JM, Iwanska A, Sommer G, et al. Repopulation of mouse liver with human hepatocytes and in vivo infection with hepatitis B virus. Hepatology 2001;33:981-988.
10. Mercer DF, Schiller DE, Elliott JF, Douglas DN, Hao C, Rinfret A, et al. Hepatitis C virus replication in mice with chimeric human livers. Nat Med 2001;7:927-933.
11. Suemizu H, Hasegawa M, Kawai K, Taniguchi K, Monnai M, Wakui M, et al. Establishment of a humanized model of liver using NOD/Shi-scid IL2Rgnull mice. Biochem Biophys Res Commun 2008;377:248-252.
12. Barshes NR, Lee TC, Udell IW, O'Mahoney CA, Karpen SJ, Carter BA, Goss JA. The Pediatric End-Stage Liver Disease (PELD) model as a predictor of survival benefit and posttransplant survival in pediatric liver transplant recipients. Liver Transpl 2006;12:475-480.
13. Weerasooriya VS, White FV, Shepherd RW. Hepatic fibrosis and survival in biliary atresia. J Pediatr 2004;144: 123-125.
14. Seglen PO. Preparation of isolated rat liver cells. Methods Cell Biol 1976;13:29-83.
15. Miyamoto Y, Suzuki S, Nomura K, Enosawa S. Improvement of hepatocyte viability after cryopreservation by supplementation of long-chain oligosaccharide in the freezing medium in rats and humans. Cell Transplant 2006;15:911-919.
16. Nakamura K, Mizutani R, Sanbe A, Enosawa S, Kasahara M, Nakagawa A, et al. Evaluation of drug toxicity with hepatocytes cultured in a micro-space cell culture system. J Biosci Bioeng 2011;111:78-84.
17. Hasegawa M, Kawai K, Mitsui T, Taniguchi K, Monnai M, Wakui M, et al. The reconstituted 'humanized liver' in TK-NOG mice is mature and functional. Biochem Biophys Res Commun 2011;405:405-410.
18. Tsukahara T, Kawaguchi S, Torigoe T, Asanuma H, Nakazawa E, Shimozawa K, et al. Prognostic significance of HLA class I expression in osteosarcoma defined by anti-pan HLA class I monoclonal antibody, EMR8-5. Cancer Sci 2006;97:1374-1380.

19. Key G, Becker MH, Baron B, Duchrow M, Schlüter C, Flad HD, Gerdes J. New Ki-67-equivalent murine monoclonal antibodies (MIB 1-3) generated against bacterially expressed parts of the Ki-67 cDNA containing three 62 base pair repetitive elements encoding for the Ki-67 epitope. Lab Invest 1993;68:629-636.

20. Scheffer GL, Kool M, Heijn M, de Haas M, Pijnenborg AC, Wijnholds J, et al. Specific detection of multidrug resistance proteins MRP1, MRP2, MRP3, MRP5, and MDR3 P-glycoprotein with a panel of monoclonal antibodies. Cancer Res 2000;60:5269-5277.

21. Dekel B, Shezen E, Even-Tov-Friedman S, Katchman H, Margalit R, Nagler A, Reisner Y. Transplantation of human hematopoietic stem cells into ischemic and growing kidneys suggests a role in vasculogenesis but not tubulogenesis. Stem Cells 2006;24:1185-1193.

22. Skalli O, Ropraz P, Trzeciak A, Benzonana G, Gillessen D, Gabbiani G. A monoclonal antibody against alpha-smooth muscle actin: a new probe for smooth muscle differentiation. J Cell Biol 1986;103(pt 2):2787-2796.

23. Hall MJ. A staining reaction for bilirubin in sections of tissue. Am J Clin Pathol 1960;34:313-316.

24. Hamada K, Monnai M, Kawai K, Nishime C, Kito C, Miyazaki N, et al. Liver metastasis models of colon cancer for evaluation of drug efficacy using NOD/Shi-scid IL2R-gammanull (NOG) mice. Int J Oncol 2008;32:153-159.

25. Limas C, Bigler A, Bair R, Bernhart P, Reddy P. Proliferative activity of urothelial neoplasms: comparison of BrdU incorporation, Ki67 expression, and nucleolar organiser regions. J Clin Pathol 1993;46:159-165.

26. Mills SJ, Shepherd NA, Hall PA, Hastings A, Mathers JC, Gunn A. Proliferative compartment deregulation in the non-neoplastic colonic epithelium of familial adenomatous polyposis. Gut 1995;36:391-394.

27. Kudo A, Kashiwagi S, Kajimura M, Yoshimura Y, Uchida K, Arii S, Suematsu M. Kupffer cells alter organic anion transport through multidrug resistance protein 2 in the post-cold ischemic rat liver. Hepatology 2004;39:1099-1109.

28. Gramignoli R, Tahan V, Dorko K, Skvorak KJ, Hansel MC, Zhao W, et al. New potential cell source for hepatocyte transplantation: discarded livers from metabolic disease liver transplants. Stem Cell Res 2013;11: 563-573.

29. Bhogal RH, Hodson J, Bartlett DC, Weston CJ, Curbishley SM, Haughton E, et al. Isolation of primary human hepatocytes from normal and diseased liver tissue: a one hundred liver experience. PLoS One 2011;6: e18222.

30. Terui K, Saito T, Hishiki T, Sato Y, Mitsunaga T, Yoshida H. Hepatic expression of multidrug resistance protein 2 in biliary atresia. Comp Hepatol 2011;10:6.

31. Pape L, Olsson K, Petersen C, von Wasilewski R, Melter M. Prognostic value of computerized quantification of liver fibrosis in children with biliary atresia. Liver Transpl 2009;15:876-882.